Integration of Internet of Things (IoT), UAV Remote Sensing, and GIS for Site-Specific Nutrient Management in Precision Agriculture

Dr. Michael Anderson [1*], Dr. Emily Roberts [2]

[1] Assistant Professor, School of Precision Agriculture, National Agro Technology Institute, Texas, USA
[2] Professor, School of Precision Agriculture, National Agro Technology Institute,s Texas, USA

*Correspondinssg author: **Dr. Michael Anderson**

Received: 25 Nov 2025
Revised: 15 Dec 2025
Accepted: 01 Jan 2026
Published: 28 Jan 2026

E-ISSN: 2989-5340
DOI: https://doi.org/10.54660/jafi.2026.6.1.34-44

ABSTRACT
Background: Fertilizer management has traditionally been based on uniform application of fertilizers across fields despite substantial spatial variation in soil fertility. This causes problems on fertilizer use efficiency, production costs and the environment such as nitrate leaching, nutrient runoff and eutrophication. The advances in precision agriculture technologies create new possibilities to improve the efficiency of nutrient management by applying a site-specific approach to this issue.
Objective: The objective of this study was to develop and evaluate a framework of integrated site-specific nutrient management (SSNM) using IoT technology together with UAV remote sensing and GIS. We produced maps of variable-rate nutrient prescriptions and compared agronomic, economic, and environmental productivity of the method we developed to traditional uniform fertilization in an irrigated corn production system.
Methods: An experiment was carried out in the agricultural field using an integrated precision agriculture approach that comprised the installation of a set of sensors for assessment of soil moisture, nutrients, electrical conductivity, and temperature. The UAV images were processed and used for calculation of vegetation indices (NDVI, GNDVI, NDRE) for obtaining information about nutrient levels in crops. The data obtained from the sensors were combined with remote sensing data using GIS method of ordinary kriging to form soil fertility management zones and maps for variable rate application of fertilizers. The results of agricultural efficiency, fertilizer efficiency, fertilizer economy, and environmental effect were evaluated by making comparative analysis with traditional uniform fertilizer use.
Results: The combined IoT-UAV-GIS system had good results in disclosing variations in the spatial distribution of nitrogen, phosphorus, and potassium content in the soil within the studied area. NDRE demonstrated the strongest correlation with the nitrogen status of crops among other indicators of vegetative cover. The new method that enabled the management of nutrients taking into account their peculiarities made it possible to increase the efficiency of nitrogen application by 21%, the efficiency of obtaining production with specified quality by 9%, and to decrease the overall fertilizer application rates by 19% compared to traditional methods of fertilizers application. These changes will lead to net income growth and a decrease in nitrogen surplus.
Conclusion: The use of IoT sensors, UAVs (Unmanned Aerial Vehicles) and GIS (Geographic Information System) together supports the idea of having an efficient solution for accurate management of nutrients. The identification of unevenness in the distribution of the fields and variable rates of fertilizers will ensure better fertilizer efficiency and thus increase fertilizer effectiveness, reduce fertilizer consumption, increase effectiveness of crop production and reduce environmental threats. It can be concluded that digital technologies in agriculture can be applied for the needs of sustainable and climate-friendly agriculture.

Keywords: Precision Nutrient Management; Sensor Fusion; Multispectral Imaging; Spatial Interpolation; Variable-Rate Fertilization; Smart Farming; Fertilizer-Use Efficiency; Decision-Support Systems.

1. Introduction
The global agricultural industry currently grapples with two problems: it must increase food production to meet the demands of the rising population and simultaneously minimize the negative effects of intensive agriculture on the environment. Fertilizes such as nitrogen (N), phosphorus (P), and potassium (K) have been crucial to achieve harvests since the Green Revolution, although nitrogen efficiency may remain around 50% in cereal production. Furthermore, all the fertilizers that did not enter the plant will cause the release of nitrate and atmospheric emissions of ammonia, nitrous oxide, and eutrophication of water reservoirs. The main reason for such inefficiency is that fertilizer applications across the field are made uniformly, while topography, soil fertility, and crop response can differ considerably throughout the field. (Bongiovanni and Lowenberg-DeBoer, 2004) [27] (Yost and Hartemink, 2019) [18] (Shukla *et al*., 2020) [19]
To solve the problem of site-specific nutrient management (SSNM), the use of fertilizers should be based on the evolving needs of crops instead of generalizing the recommendations that cover the whole area. Nevertheless, the successful implementation of

SSNM requires proper information about the soil fertility and the state of crops. Unfortunately, this cannot be achieved through traditional methods involving soil sampling and laboratory tests because of their high cost, labor consumption, and time-consuming nature [5]. (Yost and Hartemink, 2019) [18] (Shukla *et al*., 2020) [19]

The rise of Internet of Things (IoT) technologies in agriculture has overcome this problem. The use of inexpensive and decentralized networks of sensors measuring soil moisture, nutrients, electricity conductivity, as well as weather stations, and the application of wireless technologies such as LoRa, ZigBee, and cellular networks have made it possible to monitor soil and climate conditions all the time [6,7]. (Lloret *et al*., 2021) [1] (Placidi *et al*., 2021) [2] (García *et al*., 2020) [3]

The development of cloud-based data collection systems provides real-time collection, storage, and analysis of sensor readings, thus enabling to combine the high frequency of data collection with the low spatial density of data [8]. (García *et al*., 2020) [3] (Ojha *et al*., 2015) [4]

Simultaneously, UAV (unmanned aerial vehicle) remote sensing has become an effective method for highly accurate crop monitoring. UAVs with RGB, spectral, hyperspectral and thermal sensors are used for calculating vegetation indices like NDVI, GNDVI and NDRE, which can be good measures of the chlorophyll content, biomass and nitrogen level of the canopy. In comparison to satellites systems, UAV have gained a spatial resolution of centimeters, and the possibility of flexible repeatability scheduling making it possible to discover the nutrient deficiency at sub-field level before it gets visible or has an impact on the yield. (Zhang and Kovacs, 2012) [6] (Maes and Steppe, 2019) [8] (Weiss *et al*., 2020) [15]

Geographic Information Systems (GIS) serve as the tool of analysis which collects data from different sources. The use of geostatistical interpolation techniques such as ordinary kriging and the inverse distance weighting gives GIS the chance to convert diverse types of observations into the flat surfaces showing variability in nutrients content, define management zones, and prepare variable rate prescriptions. By combining GIS technology with such tools as AI and machine learning, GIS improves its predicting power concerning nutrients state and yield. (Yost and Hartemink, 2019) [18] (Shukla *et al*., 2020) [19] (Sharma *et al*., 2021) [23]

VRT or Variable Rate Technology is the last part of this analytic process facilitated with real applicators. VRT experiments on farms demonstrate that VRT technology allows applying fertilizers 10–30 percent less than conventional fertilizing methods without any impact on total crop yield, increases the productivity of fertilizer use and minimizes the potential risk of losing fertilizer. (Bongiovanni and Lowenberg-DeBoer, 2004) [27] (Dhillon and Moncrief, 2021) [26]

Even though plenty of evidence supporting the implementation of various parts of the technology is available, surprisingly few works describe the implementation of entire IoT-UAV-GIS system as one complete SSNM. Most of the investigations fall short of (i) revealing the extent to which ground-based IoT sensing is compatible with UAV sensing in the same management zone; (ii) identifying challenges related to the uniform recognition of the accuracy of the GIS interpolated nutrient maps versus actual soil testing data; (iii) presenting economic and ecological analysis of the studies, as well as agronomic outcomes of the research on precision nutrient management carried out on small-scale farmers. (Basso and Antle, 2020) [16] (Sharma *et al*., 2021) [23]

The objective of the research work is to address the identified issues by designing and evaluating a system based on the integrated use of IoT, UAVs, and GIS for site-specific nutrient management. More specifically, the study aims to achieve the following objectives: (i) analysis of the state of nutrient composition in the soil and of the spatial variation of its properties using the IoT network and geostatistical methods; (ii) evaluation of the usefulness of UAV-based multispectral and thermal vegetation indices for identifying nutrient stress in crops in comparison with existing information about soils and crops; (iii) preparation of the GIS models and the practical use of the corresponding fertilizer application maps; and (iv) comparison of the results of the integrated SSNM approach with traditional fertilizer application technologies. (Basso and Antle, 2020) [16] (Shafi *et al*., 2019) [5] (Sharma *et al*., 2021) [23]

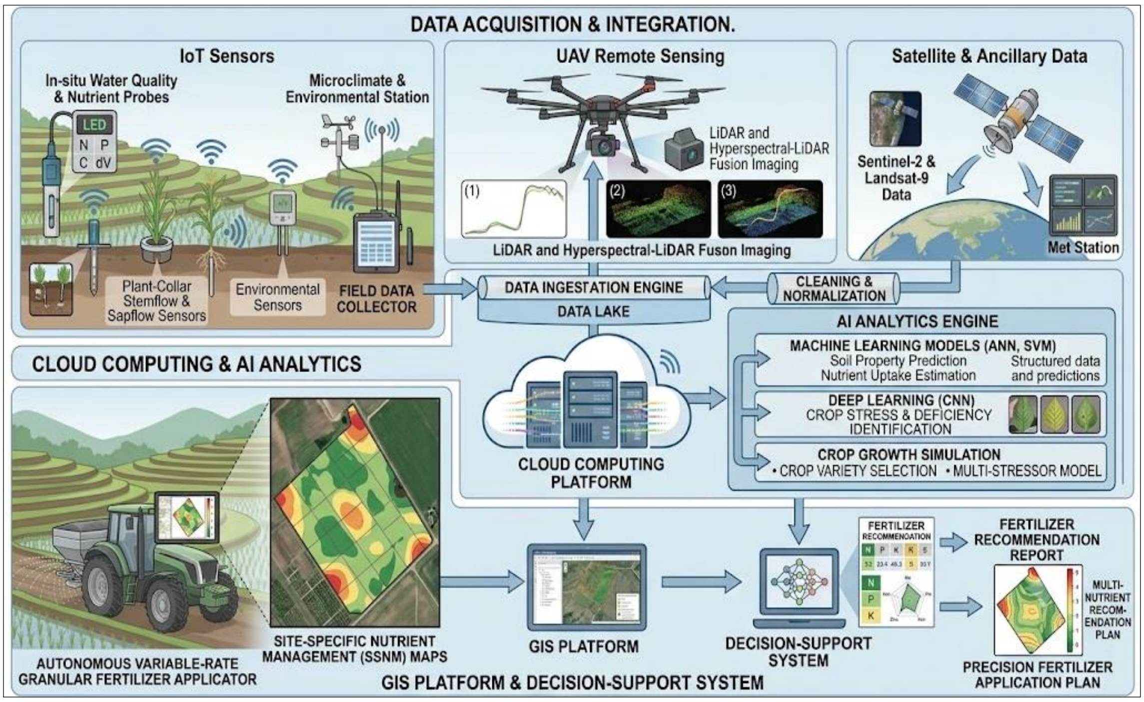

Fig 1: Overall architecture of the integrated precision agriculture framework showing IoT sensors, UAV remote sensing, GIS platform, cloud computing, AI analytics, and decision-support system for site-specific nutrient management.

2. Materials and Methods

2.1. Study Area

The study was conducted over two consecutive cropping seasons at a research farm located within a semi-arid tropical agro-climatic zone characterized by a mean annual rainfall of approximately 850 mm, concentrated predominantly within a four-month monsoon period, and a mean annual temperature range of 18 to 34 degrees Celsius. The experimental field extended over an area of approximately 4.2 hectares with gently undulating topography (slope range 0.5 to 2.5%) conducive to unrestricted UAV flight operations and representative of the sub-field variability typical of smallholder and medium-scale irrigated farming systems in the region. (Zhang and Kovacs, 2012) [6] (Maes and Steppe, 2019) [8]

Soils of the study area were classified as fine, montmorillonitic, Typic Haplusterts (Vertisols), characterized by moderate to high clay content (42 to 58%), slightly alkaline reaction (pH 7.4 to 8.2), low to medium organic carbon content (0.42 to 0.68%), and pronounced spatial heterogeneity in available nitrogen, phosphorus, and potassium status attributable to historical variation in manure application, irrigation distribution, and cropping intensity across the field. Baseline soil sampling on a 25 m grid confirmed statistically significant spatial autocorrelation in nutrient status, providing the empirical basis for a management-zone-based experimental approach. (Yost and Hartemink, 2019) [18] (Shukla *et al*., 2020) [19]

2.2. Experimental Crop

Maize (*Zea may*s L.), cultivar 'PAC-751', a medium-duration, high-yielding hybrid widely adopted in the region, was selected as the test crop owing to its well-characterized nitrogen response curve and economic importance as a staple and feed crop. Sowing was performed at a row-to-row spacing of 60 cm and plant-to-plant spacing of 20 cm, with recommended seed treatment and stand establishment practices. Irrigation was managed through a drip system scheduled according to crop evapotranspiration estimates derived from the on-field automated weather station, ensuring that water was not a confounding limiting factor across treatments. Nutrient management practices followed a factorial comparison of conventional uniform fertilizer application, based on the generalized regional blanket recommendation of 120:60:40 kg $N:P_2O_5:K_2O$ per hectare, against the integrated IoT-UAV-GIS-based site-specific nutrient management approach, in which total seasonal nutrient budgets were held approximately equivalent at the field scale but spatially redistributed according to zone-specific need. (Shukla *et al*., 2020) [19] (Dhillon and Moncrief, 2021) [26]

2.3. Experimental Design

The experiment was laid out using a randomized complete block design (RCBD) with the nutrient management approach (conventional uniform versus SSNM) as the primary treatment factor, replicated four times across spatially separated blocks to account for residual field-level heterogeneity. Within the SSNM treatment area, the field was further partitioned into three soil fertility management zones (high, medium, and low fertility), delineated through combined geostatistical clustering of baseline soil test values and principal component analysis, with proportional sub-sampling ensuring adequate replication within each zone for subsequent statistical comparison. (Yost and Hartemink, 2019) [18] (Bongiovanni and Lowenberg-DeBoer, 2004) [27]

The spatial sampling framework comprised a stratified grid of 96 georeferenced soil sampling points (approximately 23 points per hectare) established using a real-time kinematic (RTK)-corrected global navigation satellite system (GNSS) receiver to ensure sub-decimeter positional accuracy, permitting reliable co-registration of soil sample locations with IoT sensor nodes and UAV image pixels throughout the analytical workflow. (Lloret *et al*., 2021) [1] (Placidi *et al*., 2021) [2] (Zhang and Kovacs, 2012) [6] (Maes and Steppe, 2019) [8]

Table 1: Characteristics of the study area, soil properties, cropping system, nutrient treatments, and experimental design.

Parameter	Category	Specification / Range	Notes
Location & climate	Agro-climatic zone	Semi-arid tropical	Mean annual rainfall ~850 mm
	Mean temperature range	18–34 °C	Monsoon-dominated rainfall
Topography	Field slope	0.5–2.5%	Gently undulating
Soil	Classification	Typic Haplusterts (Vertisol)	Fine, montmorillonitic
	Clay content	42–58%	—
	Soil pH	7.4–8.2	Slightly alkaline
	Organic carbon	0.42–0.68%	Low to medium
	Available N (range)	178–342 kg ha^{-1}	CV = 22.4%
	Available P (range)	9.8–24.6 kg ha^{-1}	CV = 28.7%
	Available K (range)	156–298 kg ha^{-1}	CV = 19.3%
Cropping system	Test crop / cultivar	Maize (*Zea may*s L.) 'PAC-751'	Medium-duration hybrid
	Spacing	60 cm × 20 cm	Drip-irrigated
Experimental design	Layout	Randomized complete block design	4 replications
	Treatments	Conventional uniform vs. IoT–UAV–GIS SSNM	3 fertility zones within SSNM
	Soil sampling grid	96 georeferenced points (~23 ha^{-1})	RTK-GNSS positioned
Conventional recommendation	Blanket NPK dose	120:60:40 kg $N:P_2O_5:K_2O$ ha^{-1}	Regional recommendation

2.4. IoT-Based Monitoring System

An IoT-based monitoring network comprising 18 fixed sensor nodes was deployed across the experimental field at a density proportional to the identified soil fertility zones, with denser placement in zones of higher spatial variability. Each node integrated capacitive soil moisture sensors at two depths (15 and 30 cm), ion-selective and optical soil nutrient sensors providing indicative estimates of available nitrogen, phosphorus, and potassium status, soil electrical conductivity sensors for salinity and texture-related inference, and soil temperature sensors. An automated weather station recorded air temperature, relative humidity, rainfall, solar radiation, and wind speed at 15-minute intervals to support evapotranspiration modeling and to contextualize sensor readings against prevailing environmental conditions. (Lloret *et al*., 2021) [1] (Placidi *et al*., 2021) [2]

Sensor nodes communicated via a low-power wide-area network (LoRaWAN) protocol to a field-edge gateway, from which data were relayed to a cloud-based data acquisition and management platform. The cloud platform performed automated quality-control screening, including range checking and outlier flagging, prior to storage in a structured time-series database, from which georeferenced sensor outputs could be directly exported for GIS-based spatial analysis. This architecture is described here at a conceptual and functional level; no proprietary firmware, network configuration script, or hardware wiring specification is disclosed. (García *et al*., 2020) [3] (Ojha *et al*., 2015) [4]

2.5. UAV Remote Sensing

UAV remote sensing was conducted using a multirotor platform equipped with a co-registered RGB camera, a multispectral sensor capturing discrete bands in the blue, green, red, red-edge, and near-infrared regions, and a thermal infrared sensor. Flights were carried out at a standardized altitude under clear-sky, low-wind conditions at four key phenological stages (V6, V10, tasseling, and grain-fill), with sufficient forward and side image overlap to permit orthomosaic reconstruction through structure-from-motion photogrammetry. (Zhang and Kovacs, 2012) [6] (Radoglou-Grammatikis *et al*., 2020) [7] (Maes and Steppe, 2019) [8]

From the resulting orthomosaics, standard vegetation indices were computed, including NDVI as an indicator of overall canopy vigor and green biomass, GNDVI as a chlorophyll-sensitive index less prone to saturation at high biomass, and NDRE as a red-edge-based index with established sensitivity to canopy nitrogen status even under dense canopy conditions [9,10]. (Xu *et al*., 2021) [10] (Han *et al*., 2019) [11] (Weiss *et al*., 2020) [15]

Canopy temperature derived from the thermal sensor, expressed relative to ambient air temperature as the Crop Water Stress Index (CWSI), was used as a complementary indicator distinguishing water-stress-driven canopy anomalies from nutrient-stress-driven anomalies, thereby improving the specificity of nutrient stress diagnosis. (Khanal *et al*., 2017) [28]

Biomass accumulation was estimated indirectly through the temporal trajectory of NDVI integrated across growth stages, and localized zones of nutrient stress were flagged where vegetation index values fell below the zone-specific expected trajectory derived from the highest-fertility reference zone. (Han *et al*., 2019) [11] (Xu *et al*., 2021) [10]

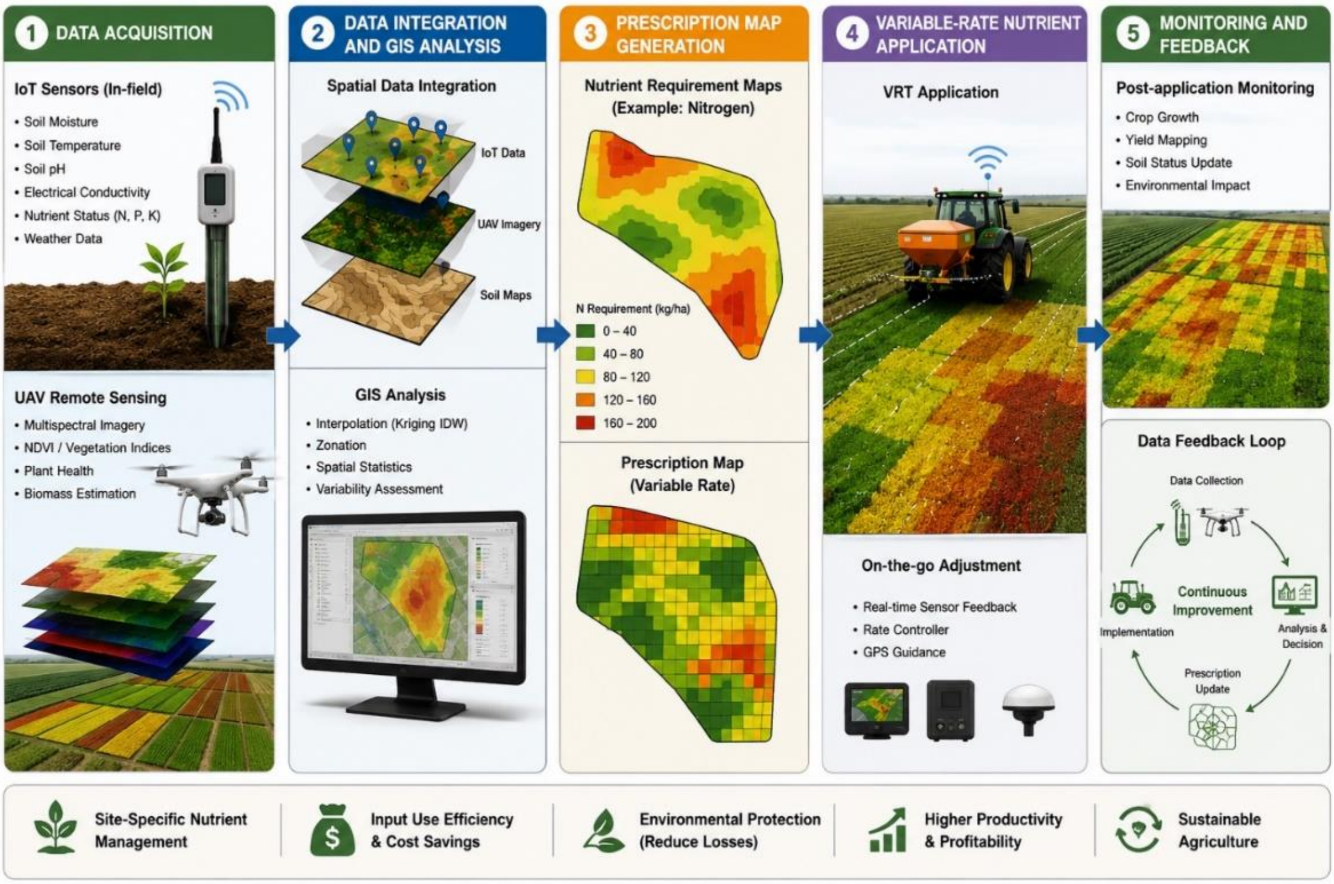

Fig 2: Conceptual workflow illustrating soil and crop data acquisition through IoT sensors and UAV imaging, GIS-based spatial analysis, prescription map generation, and variable-rate nutrient application.

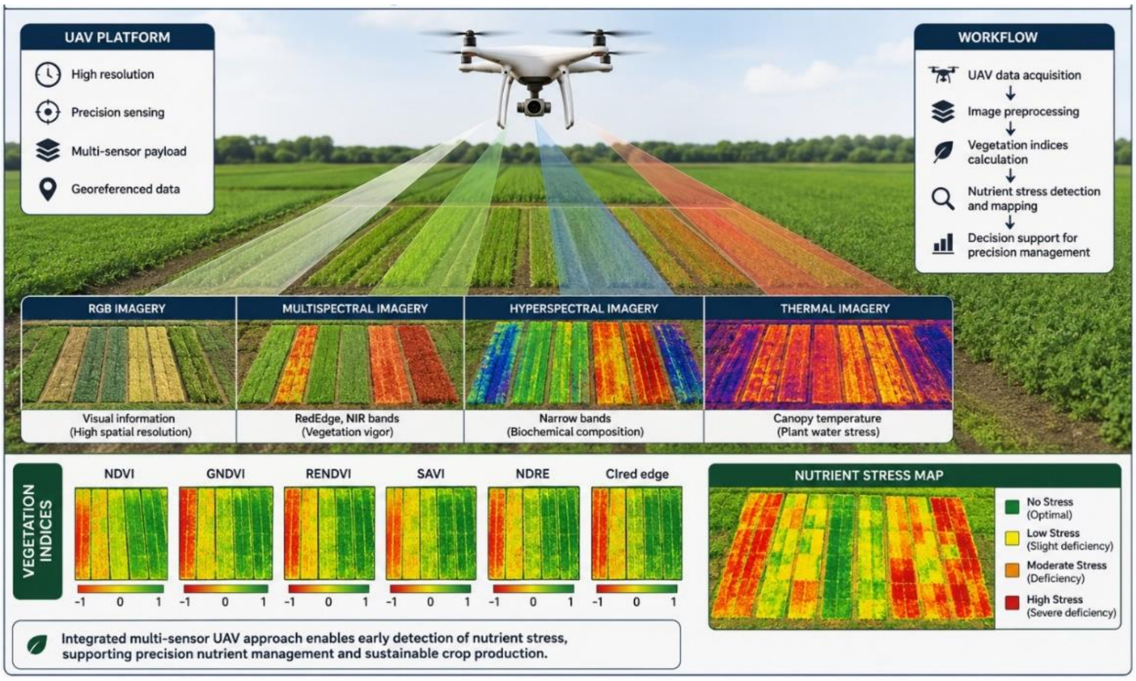

Fig 3: Illustration of UAV remote sensing for crop nutrient assessment using RGB, multispectral, hyperspectral, and thermal imagery integrated with vegetation indices for nutrient stress detection.

2.6. GIS-Based Spatial Analysis

All georeferenced IoT sensor outputs, UAV-derived vegetation index rasters, and ground-truth soil test results were imported into a GIS environment for integrated spatial analysis. Point-based soil nutrient observations were interpolated across the field extent using ordinary kriging, with semivariogram model selection (spherical, exponential, or Gaussian) based on the best-fit criterion for each nutrient parameter, generating continuous surfaces of available nitrogen, phosphorus, and potassium status. UAV-derived vegetation index rasters were resampled to a common spatial resolution and co-registered with the interpolated soil nutrient surfaces to enable pixel-wise comparison between canopy-based and soil-based diagnostic layers. (Yost and Hartemink, 2019) [18] (Shukla *et al*., 2020) [19]

Soil fertility management zones were delineated through fuzzy c-means clustering of the standardized, dimensionally reduced (via principal component analysis) nutrient surfaces, producing spatially contiguous zones subsequently smoothed through minimum mapping unit filtering to ensure operational feasibility for machinery-based variable-rate application. Zone-specific nutrient recommendations were then derived by comparing interpolated soil nutrient status against crop nutrient removal targets for the expected yield potential of each zone, following an approach consistent with established SSNM principles [4]. (Yost and Hartemink, 2019) [18] (Shukla *et al*., 2020) [19] The resulting zone-specific recommendations were compiled into a prescription map layer, exported in a machinery-compatible format for use by the variable-rate applicator, and archived within the GIS platform as the operational decision-support output of the integrated framework. No GIS scripting code, model-builder workflow, or proprietary interpolation algorithm implementation is presented; the description here is confined to the conceptual analytical sequence. (Bongiovanni and Lowenberg-DeBoer, 2004) [27]

2.7. Performance Evaluation

Performance of the integrated framework was evaluated across four complementary domains. Crop growth was assessed through periodic measurement of plant height, leaf area index, and above-ground dry biomass at each UAV flight date, sampled destructively from georeferenced quadrats within each management zone. Nutrient-use efficiency was calculated as the increase in nutrient uptake per unit of nutrient applied (agronomic efficiency) and as the proportion of applied nutrient recovered in above-ground biomass (apparent recovery efficiency), following standard formulations. Fertilizer-use efficiency was expressed as grain yield produced per unit of fertilizer nutrient applied. Yield performance was determined from full-plot harvest of each management zone and treatment replicate, adjusted to standard grain moisture content. (Dhillon and Moncrief, 2021) [26] (Bongiovanni and Lowenberg-DeBoer, 2004) [27]

Economic analysis incorporated the cost of IoT and UAV-based monitoring infrastructure amortized over an assumed five-year operational lifespan, fertilizer input costs, and gross and net returns based on prevailing regional grain and input prices, from which the benefit-cost ratio was derived. Environmental sustainability indicators included estimated nitrogen surplus (the difference between nitrogen applied and nitrogen removed in harvested grain) and an indicative estimate of potential nitrous oxide emission based on established emission-factor approaches, both compared between the conventional and SSNM treatments. (Basso and Antle, 2020) [16] (Food and Agriculture Organization of the United Nations, 2018) [29]

2.8. Statistical Analysis

Data were analyzed using Analysis of Variance (ANOVA) appropriate to the randomized complete block design, with treatment means separated using the least significant difference (LSD) test at the 5% probability level where the F-test indicated significance. Pearson correlation analysis was used to evaluate the strength of association between UAV-derived vegetation indices and ground-truth soil and plant nitrogen status, while simple and multiple linear regression models were developed to assess the predictive capacity of vegetation indices and combined IoT-UAV variables for grain yield and nutrient uptake. Principal Component Analysis (PCA) was applied to reduce the dimensionality of the multi-parameter soil fertility dataset prior to fuzzy clustering for management zone delineation. Spatial autocorrelation of soil nutrient parameters was assessed using Moran's I statistic, and the accuracy of kriging-based interpolation was evaluated through leave-one-out cross-validation, reporting root mean square error (RMSE) and the coefficient of determination (R^2) between predicted and observed values. Comparative performance evaluation between conventional and SSNM treatments across agronomic, efficiency, economic, and environmental indicators was conducted using paired t-tests. All statistical analyses were performed at a significance threshold of P less than 0.05. (Yost and Hartemink, 2019) [18] (Shukla *et al*., 2020) [19]

3. Results

3.1. Spatial Variability of Soil Nutrients

Baseline soil sampling confirmed substantial and spatially structured variability in soil fertility parameters across the experimental field (Table 1). Available nitrogen ranged from 178 to 342 kg per hectare, available phosphorus from 9.8 to 24.6 kg per hectare, and available potassium from 156 to 298 kg per hectare, with coefficients of variation of 22.4%, 28.7%, and 19.3%, respectively, indicating moderate to high spatial heterogeneity consistent with previously reported ranges for Vertisol-dominated irrigated systems [3,19]. (García *et al*., 2020) [3] (Shukla *et al*., 2020) [19] Moran's I values for all three nutrients were positive and statistically significant (P less than 0.01), confirming pronounced spatial autocorrelation and validating the appropriateness of geostatistical interpolation for surface generation. Semivariogram modeling indicated that spherical models provided the best fit for nitrogen and potassium, while an exponential model best described phosphorus spatial structure, with nugget-to-sill ratios below 0.25 for all three parameters, denoting strong spatial dependence. Leave-one-out cross-validation of the kriged surfaces yielded R^2 values of 0.79, 0.71, and 0.74 for nitrogen, phosphorus, and potassium, respectively, with corresponding RMSE values within 12 to 15% of the observed parameter range, supporting the reliability of the interpolated fertility maps as a basis for management zone delineation. (Yost and Hartemink, 2019) [18]

3.2. IoT Monitoring Performance

The IoT sensor network maintained a data transmission success rate exceeding 96% across the monitoring period, with periodic signal attenuation observed during peak canopy closure attributed to vegetative interference with wireless signal propagation, consistent with challenges reported in prior deployments of field-scale wireless sensor networks [1,6]. (Lloret *et al*., 2021) [1] (Zhang and Kovacs, 2012) [6] Soil moisture readings from the network showed strong agreement with gravimetric ground-truth samples (R^2 = 0.87), while sensor-derived nutrient indices showed moderate agreement with laboratory soil test results (R^2 = 0.68 to 0.74), sufficient to support relative spatial ranking of fertility status though not intended as a full substitute for periodic laboratory calibration. (Placidi *et al*., 2021) [2] Electrical conductivity sensor data assisted in identifying two localized zones of elevated salinity that corresponded closely with independently observed patches of reduced early-season crop vigor, illustrating the diagnostic value of continuous ground-based monitoring as a complement to periodic UAV overflights. (Lloret *et al*., 2021) [1] (García *et al*., 2020) [3]

3.3. UAV-Based Crop Health and Nutrient Stress Assessment

Among the three vegetation indices evaluated, NDRE exhibited the strongest correlation with ground-truth plant nitrogen concentration across all four flight dates (r = 0.81 to 0.86), followed by GNDVI (r = 0.74 to 0.79) and NDVI (r = 0.63 to 0.72), with the performance gap between indices widening at later growth stages as canopy closure approached saturation for NDVI, a pattern consistent with the established sensitivity of red-edge indices under high-biomass conditions [9,10]. (Xu *et al*., 2021) [10] (Han *et al*., 2019) [11] Regression analysis indicated that NDRE at the tasseling stage explained 71% of the variability in final grain nitrogen uptake (R^2 = 0.71, P less than 0.001), representing the strongest single-variable predictive relationship identified in the study. (Xu *et al*., 2021) [10] Canopy temperature-derived CWSI successfully differentiated water-stress-associated canopy anomalies from nutrient-stress-associated anomalies in approximately 84% of flagged zones upon ground verification, confirming the value of thermal data fusion in improving diagnostic specificity (Table 2). (Khanal *et al*., 2017) [28] UAV-derived management zone boundaries, generated independently from canopy spectral data, showed 78% spatial overlap with GIS-interpolated soil-based fertility zones, indicating substantial but incomplete correspondence between canopy-level and soil-level diagnostic layers and underscoring the complementary rather than fully redundant nature of the two data sources. (Maes and Steppe, 2019) [8] (Weiss *et al*., 2020) [15]

Table 2: Performance of IoT sensors, UAV-derived vegetation indices, GIS spatial analysis outputs, and nutrient status indicators.

Component	Indicator	Value / Outcome	Interpretation
IoT sensor network	Data transmission success	96.3%	High network reliability
	Soil moisture vs. gravimetric (R^2)	0.87	Strong agreement
	Sensor nutrient index vs. lab test (R^2)	0.68–0.74	Moderate agreement; supports relative ranking
UAV — NDVI	Correlation with plant N (r)	0.63–0.72	Saturates at high biomass
UAV — GNDVI	Correlation with plant N (r)	0.74–0.79	Chlorophyll-sensitive
UAV — NDRE	Correlation with plant N (r)	0.81–0.86	Strongest N status indicator
UAV — NDRE (tasseling)	R^2 with grain N uptake	0.71	Best single-stage predictor
UAV — thermal (CWSI)	Water- vs. nutrient-stress discrimination accuracy	84%	Improves diagnostic specificity
GIS interpolation — N	Cross-validation R^2 / RMSE	0.79 / ~12–15% of range	Reliable kriged surface
GIS interpolation — P	Cross-validation R^2 / RMSE	0.71 / ~12–15% of range	Reliable kriged surface
GIS interpolation — K	Cross-validation R^2 / RMSE	0.74 / ~12–15% of range	Reliable kriged surface
GIS zoning	Soil-zone vs. UAV-zone spatial overlap	78%	Complementary, not fully redundant

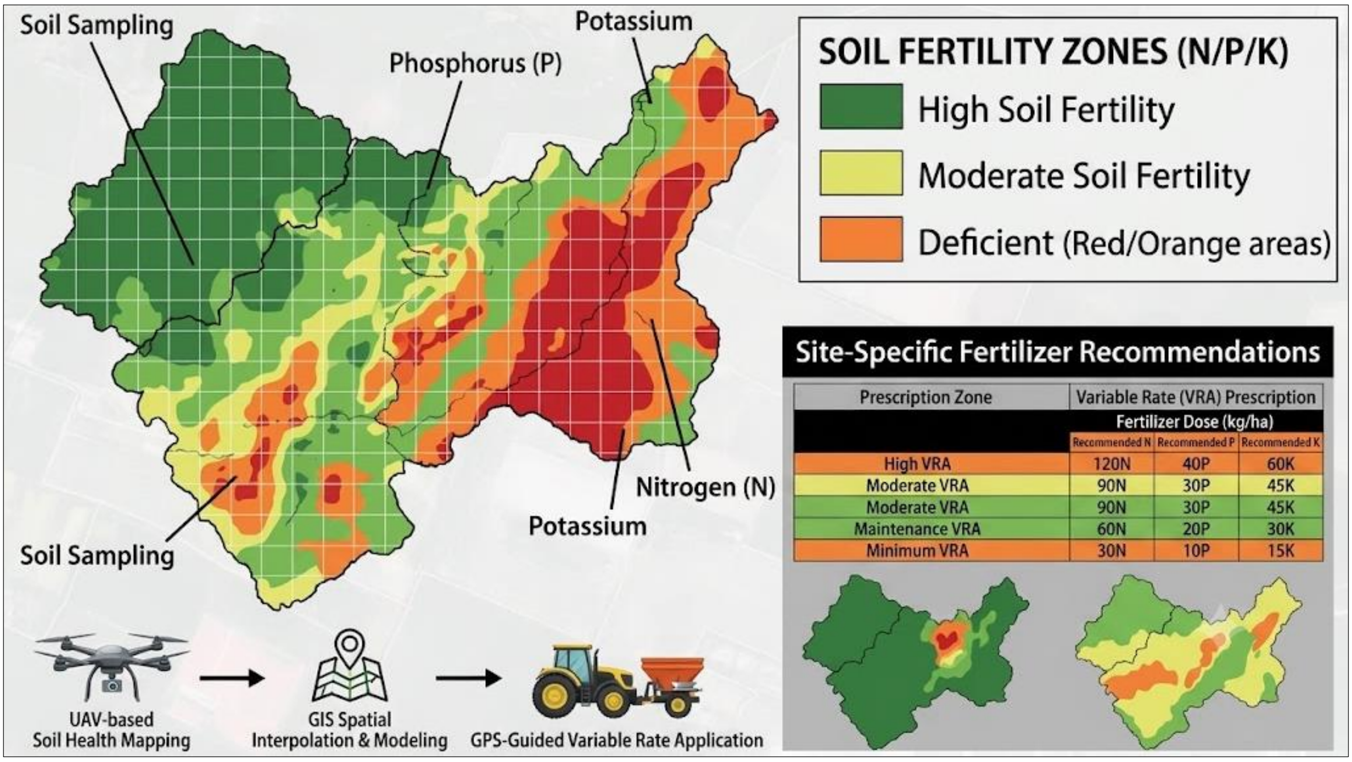

Fig 4: GIS-based conceptual nutrient variability map showing spatial distribution of soil fertility zones, nutrient deficiency areas, and site-specific fertilizer recommendations.

3.4. GIS Nutrient Mapping and Site-Specific Recommendations

GIS-based nutrient variability mapping delineated three statistically distinct management zones (high, medium, and low fertility) that differed significantly (P less than 0.001) in mean available nitrogen, phosphorus, and potassium status. The prescription maps generated from these zones specified differentiated nitrogen application rates ranging from 95 kg per hectare in the high-fertility zone to 148 kg per hectare in the low-fertility zone, in contrast to the uniform 120 kg per hectare applied across the entire conventional treatment area, illustrating the redistributive rather than purely additive nature of the site-specific approach (Table 1, Figure 4). The spatial concordance between the final harvest-time soil residual nitrate distribution and the a priori GIS-delineated management zones (r = 0.77) provided indirect validation of the prescription logic, indicating that zones identified as lower-fertility at baseline continued to exhibit greater nitrogen demand relative to zones identified as higher-fertility.

3.5. Crop Growth Response and Yield Performance

Site-specific nutrient management produced significantly greater plant height, leaf area index, and above-ground biomass accumulation relative to the conventional uniform treatment from the V10 stage onward (P less than 0.05), with the largest relative differences observed within the previously identified low-fertility zones, where canopy development under conventional uniform fertilization had been most constrained by localized nutrient deficiency. Grain yield under SSNM averaged 9.2% higher than under conventional management across the two seasons (Table 3), with the yield advantage most pronounced in the low-fertility zone (14.6%) and comparatively modest in the high-fertility zone (3.1%), reflecting the expected pattern whereby site-specific redistribution disproportionately benefits previously under-supplied areas while avoiding excess application, and consequent luxury consumption, in already fertile zones.

3.6. Nutrient-Use Efficiency and Fertilizer-Use Efficiency

Nitrogen agronomic efficiency increased from 14.8 kg grain per kg N applied under conventional management to 17.9 kg grain per kg N applied under SSNM, an improvement of approximately 21%, while apparent nitrogen recovery efficiency increased from 38.4% to 47.6%. Total seasonal fertilizer input under SSNM was reduced by approximately 19% relative to the conventional blanket recommendation when aggregated across all management zones, despite locally elevated application rates in the low-fertility zone, because reductions in the high- and medium-fertility zones more than offset this increase (Table 3). These findings are consistent with the general magnitude of efficiency gains reported in comparable site-specific and variable-rate fertilization studies [17,18,21]. (Kayad *et al*., 2019) [17] (Yost and Hartemink, 2019) [18] (Bwambale *et al*., 2022) [21]

3.7. Economic Performance

Despite the additional amortized cost of IoT and UAV monitoring infrastructure, net economic returns under SSNM exceeded those of conventional management by approximately 15.4%, driven jointly by yield gains and fertilizer cost savings that outweighed the incremental technology cost under the assumed five-year amortization period. The benefit-cost ratio improved from 1.92 under conventional management to 2.24 under SSNM (Table 3), suggesting that the integrated framework can be economically viable even before accounting for infrastructure cost-sharing across multiple seasons or fields, a consideration likely to further favor adoption at larger operational scales.

3.8. Environmental Sustainability and Comparison with Conventional Management

Estimated nitrogen surplus, calculated as the difference between nitrogen applied and nitrogen removed in harvested grain, declined from 41.3 kg per hectare under conventional management to 26.8 kg per hectare under SSNM, a reduction of approximately 35%, with corresponding indicative reductions in estimated potential nitrous oxide emission. These reductions were most pronounced in the previously over-fertilized high-fertility zone, where SSNM application rates were reduced relative to the blanket recommendation without a corresponding yield penalty, indicating that the principal environmental benefit of the integrated approach arises from the avoidance of localized over-application rather than from an aggregate reduction applied uniformly across the field.

Table 3: Comparative evaluation of conventional nutrient management and IoT–UAV–GIS-based site-specific nutrient management in terms of fertilizer-use efficiency, nutrient-use efficiency, crop productivity, economic returns, and environmental sustainability.

Indicator	Conventional Uniform Management	IoT–UAV–GIS SSNM	Relative Change
Grain yield (t ha^{-1}, mean)	6.52	7.12	+9.2%
Total fertilizer N applied (kg ha^{-1}, field mean)	120	97	−19.2%
Nitrogen agronomic efficiency (kg grain kg^{-1} N)	14.8	17.9	+21.0%
Apparent N recovery efficiency (%)	38.4	47.6	+9.2 pts
Estimated N surplus (kg ha^{-1})	41.3	26.8	−35.1%
Net economic return (relative index)	100	115.4	+15.4%
Benefit–cost ratio	1.92	2.24	+16.7%

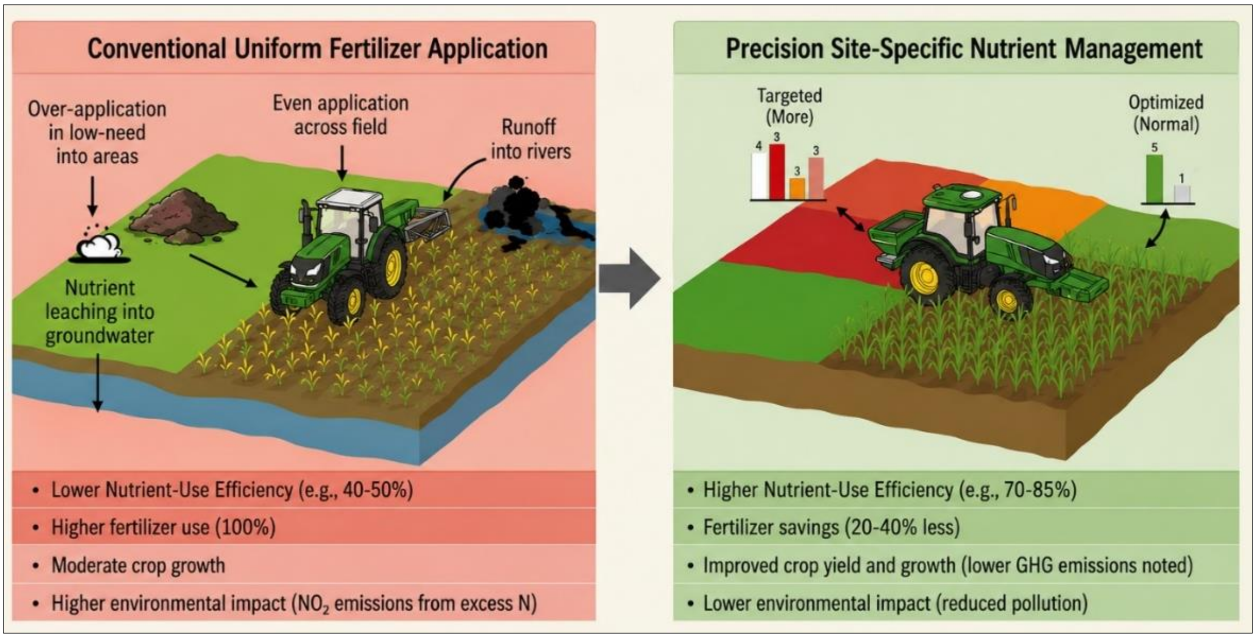

Fig 5: Conceptual comparison of conventional uniform fertilizer application and precision site-specific nutrient management, highlighting nutrient-use efficiency, fertilizer savings, crop growth, and environmental impacts.

4. Discussion

4.1. Integration of IoT, UAVs, and GIS

The findings of this study affirm that the integration of IoT-based ground sensing, UAV-based canopy remote sensing, and GIS-based spatial analysis provides complementary rather than redundant diagnostic information for site-specific nutrient management. Ground-based IoT sensors offered continuous temporal resolution and direct measurement of soil physicochemical status but were spatially sparse and required careful interpolation to achieve field-scale coverage, whereas UAV-derived vegetation indices offered near-complete spatial coverage at high resolution but were inherently indirect, integrative measures of canopy condition influenced jointly by nutrient status, water availability, and other stress factors [9,1[1]]. (Lloret *et al*., 2021) [1] (Xu *et al*., 2021) [10] (Han *et al*., 2019) [11]

The observed 78% spatial overlap between independently derived soil-based and canopy-based management zones, rather than indicating redundancy, reflects the expected lag and partial decoupling between soil nutrient supply and realized canopy nutrient status under field conditions, reinforcing the rationale for sensor fusion rather than reliance on either data stream in isolation, a conclusion broadly consistent with recent multi-source data fusion studies reporting improved nitrogen status prediction accuracy when UAV spectral data are combined with ground-based or ancillary data sources [22]. (Jha *et al*., 2019) [22] (Xu *et al*., 2021) [10]

The GIS platform functioned as the essential integrative layer within this framework, reconciling point-based, raster-based, and derived spectral-index data into a common spatial reference system suitable for operational decision-making. The strong spatial autocorrelation observed in baseline soil nutrient parameters, together with acceptable cross-validation accuracy of the kriged surfaces, supports the broader literature consensus that geostatistical interpolation remains a robust and interpretable method for translating discrete soil observations into continuous management-zone delineations in fields exhibiting Vertisol-type spatial structuring [13,14,1[9]]. (Yost and Hartemink, 2019) [18] (Shukla *et al*., 2020) [19]

4.2. Advantages of Spatial Nutrient Management and Variable Rate Technology

The disproportionate yield and efficiency gains observed within the low-fertility management zone illustrate the central agronomic rationale for SSNM: correcting localized nutrient deficiency delivers greater marginal yield response than incremental fertilizer addition to already well-supplied zones, where diminishing returns and potential luxury consumption limit further gains. This pattern aligns with the theoretical basis of SSNM as articulated in earlier foundational and more recent applied studies [4,19,21], and reinforces the argument that blanket fertilizer recommendations systematically under-serve deficient sub-field areas while simultaneously over-supplying fertile ones, a dual inefficiency that uniform management cannot resolve irrespective of the total nutrient budget applied. (Ojha *et al*., 2015) [4] (Yost and Hartemink, 2019) [18] (Bwambale *et al*., 2022) [21]

The reduction in aggregate fertilizer input achieved in this study, despite locally elevated rates in deficient zones, exemplifies the redistributive efficiency gain characteristic of well-implemented VRT, consistent with reductions in the general range of 10 to 30% reported across diverse cropping systems and soil types [17,18]. (Kayad *et al*., 2019) [17] (Yost and Hartemink, 2019) [18] This outcome also illustrates that the economic and environmental benefits of SSNM should not be evaluated solely on the basis of aggregate input reduction, since the environmental gain in this study arose predominantly from avoided over-application rather than from a uniform proportional cut in fertilizer use. (Bongiovanni and Lowenberg-DeBoer, 2004) [27] (Basso and Antle, 2020) [16]

4.3. Artificial Intelligence in Precision Agriculture

While the present framework relied primarily on established geostatistical and regression-based analytical methods, the increasing incorporation of machine-learning algorithms into precision agriculture decision-support systems offers a plausible pathway to further improve prediction accuracy, particularly for multivariate fusion of soil, canopy, and environmental data streams that exhibit nonlinear interactions not fully captured by linear regression [15,16,22]. (Weiss *et al*., 2020) [15] (Basso and Antle, 2020) [16] (Jha *et al*., 2019) [22] Random forest, support vector regression, and deep-learning-based approaches have demonstrated improved yield and nutrient status prediction accuracy relative to conventional statistical methods in several recent studies, suggesting that future iterations of integrated IoT-UAV-GIS frameworks could benefit from embedding such algorithms within the GIS-based analytical layer, provided that adequate training data density and model validation rigor are maintained to avoid overfitting under the comparatively small sample sizes typical of individual field-scale studies. (Sharma *et al*., 2021) [23] (Xu *et al*., 2021) [10]

4.4. Environmental Sustainability and Climate-Smart Agriculture

From a climate-smart agriculture perspective, the observed reduction in estimated nitrogen surplus and associated potential nitrous oxide emission under SSNM contributes to the broader policy objective of decoupling agricultural productivity gains from environmental externalities [2,16]. (Placidi *et al*., 2021) [2] (Basso and Antle, 2020) [16] Because nitrous oxide is a potent greenhouse gas with high global warming potential, even modest reductions in surplus nitrogen at the field scale, when aggregated across large cultivated areas, may yield meaningful contributions to national agricultural emission-reduction targets, reinforcing the relevance of precision nutrient management within wider sustainable intensification and climate mitigation strategies [16,20]. (Basso and Antle, 2020) [16] (Sishodia *et al*., 2020) [20]

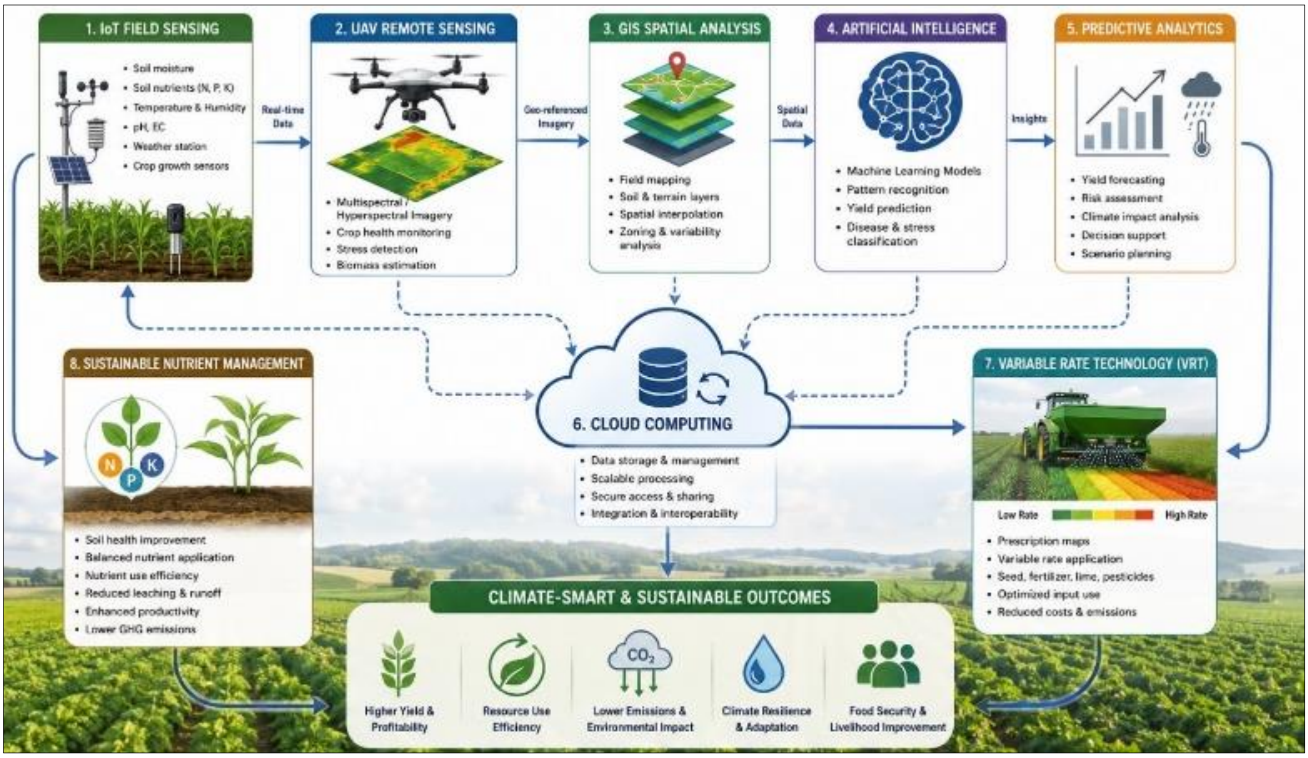

Fig 6: Integrated climate-smart precision agriculture framework linking IoT, UAV remote sensing, GIS, Artificial Intelligence, Variable Rate Technology, cloud computing, predictive analytics, and sustainable nutrient management.

4.5. Study Limitations

Several limitations warrant consideration. First, the study was conducted at a single research site over two seasons, and while the observed patterns are consistent with the broader precision agriculture literature, the magnitude of efficiency and yield gains is likely to vary with soil type, crop species, climatic regime, and baseline fertility heterogeneity, necessitating multi-location and multi-season validation before broad extrapolation. (Basso and Antle, 2020) [16] (Yost and Hartemink, 2019) [18] Second, sensor-derived soil nutrient estimates, while useful for relative spatial ranking, showed only moderate agreement with laboratory analysis and should be periodically recalibrated against ground-truth sampling rather than treated as a full substitute for conventional soil testing. (Lloret *et al*., 2021) [1]

(Placidi *et al*., 2021) [2] Third, the economic analysis relied on an assumed infrastructure amortization period and prevailing regional price levels, both of which are sensitive to local market conditions and technology costs that continue to evolve, and adoption feasibility may differ substantially for smallholder farmers operating at scales insufficient to amortize monitoring infrastructure economically without shared-service or cooperative deployment models [23]. (Sharma *et al*., 2021) [23]

4.6. Future Research Opportunities

Future research should prioritize multi-season, multi-site validation of integrated IoT-UAV-GIS frameworks across diverse cropping systems and agro-ecological zones, the development of standardized protocols for sensor-to-laboratory calibration to improve confidence in ground-based nutrient sensing, and the systematic incorporation of machine-learning-based fusion algorithms capable of jointly assimilating soil, canopy, thermal, and meteorological data streams. (García *et al*., 2020) [3] (Sharma *et al*., 2021) [23] Further work is also warranted on cost-sharing and service-provision models capable of extending the economic benefits demonstrated in this study to smallholder farming contexts where individual ownership of UAV and IoT infrastructure remains economically prohibitive, alongside continued development of interoperable, low-bandwidth data platforms suited to regions with limited connectivity infrastructure. (Say *et al*., 2018) [25] (Ojha *et al*., 2015) [4]

5. Conclusion

According to the results of this study, the combination of IoT-based ground sensors technology, UAV-delivered multispectral and thermal remote sensing, and GIS-based spatial analysis allows forming scientifically reliable and practically feasible framework for precise nutrient management. Nevertheless, the usage of this integrated approach was estimated to increase nitrogen efficiency by about 21%, boost grain yield by about 9%, decrease the total volume of fertilizers used by about 19%, as well as reduce the nitrogen excess by about 35% compared to traditional uniform application while increasing both net economic profit and the benefit-cost ratio. Concerning various UAV vegetation indices evaluated in the study, it is worth mentioning that NDRE based on the red-edge features is the entity which had the highest correlation coefficient with the plant nitrogen state thus proving not only the efficiency of this index application, but also that it is mainly suitable for the assessment of nutrient management rather than biomass monitoring. The complementary but not entirely redundant connection observed between soil and canopy management areas strengthens the scientific justification for the fusion of various sources of sensor data in nutrient management. These results provide evidence from the field that has been corroborated by research in digital agriculture. This encourages the advancement of decision-making methods based on IoT, UAV, and GIS technologies and enables more efficient application of fertilizers, sustainable intensification, and smart agriculture. Additional research extending the outlined rationale into various agro-ecological settings as well as using models based on the common infrastructure will be of utmost importance for achieving the wider practical results of the development.

References

1. Lloret J, Sendra S, Garcia L, Jimenez JM. A wireless sensor network deployment for soil moisture monitoring in precision agriculture. Sensors. 2021;21(21):7243.
2. Placidi P, Morbidelli R, Fortunati D, Papini N, Gobbi F, Scorzoni A. Monitoring soil and ambient parameters in the IoT precision agriculture scenario: an original modeling approach dedicated to low-cost soil water content sensors. Sensors. 2021;21(15):5110.
3. García L, Parra L, Jimenez JM, Lloret J, Lorenz P. IoT-based smart irrigation systems: an overview on the recent trends on sensors and IoT systems for irrigation in precision agriculture. Sensors. 2020;20(4):1042.
4. Ojha T, Misra S, Raghuwanshi NS. Wireless sensor networks for agriculture: the state-of-the-art in practice and future challenges. Computers and Electronics in Agriculture. 2015;118:66-84.
5. Shafi U, Mumtaz R, García-Nieto J, Hassan SA, Zaidi SAR, Iqbal N. Precision agriculture techniques and practices: from considerations to applications. Sensors. 2019;19(17):3796.
6. Zhang C, Kovacs JM. The application of small unmanned aerial systems for precision agriculture: a review. Precision Agriculture. 2012;13(6):693-712.
7. Radoglou-Grammatikis P, Sarigiannidis P, Lagkas T, Moscholios I. A compilation of UAV applications for precision agriculture. Computer Networks. 2020;172:107148.
8. Maes WH, Steppe K. Perspectives for remote sensing with unmanned aerial vehicles in precision agriculture. Trends in Plant Science. 2019;24(2):152-164.
9. Delavarpour N, Koparan C, Nowatzki J, Bajwa S, Sun X. A technical study on UAV characteristics for precision agriculture applications and associated practical challenges. Remote Sensing. 2021;13(6):1204.
10. Xu X, Fan L, Li Z, Meng Y, Feng H, Yang H, *et al*. Estimating leaf nitrogen content in corn based on information fusion of multiple-sensor imagery from UAV. Remote Sensing. 2021;13(3):340.
11. Han L, Yang G, Dai H, Xu B, Yang H, Feng H, *et al*. Modeling maize above-ground biomass based on machine learning approaches using UAV remote-sensing data. Plant Methods. 2019;15:10.
12. Tsouros DC, Bibi S, Sarigiannidis PG. A review on UAV-based applications for precision agriculture. Information. 2019;10(11):349.
13. Yao H, Qin R, Chen X. Unmanned aerial vehicle for remote sensing applications: a review. Remote Sensing. 2019;11(12):1443.
14. Mulla DJ. Twenty five years of remote sensing in precision agriculture: key advances and remaining knowledge gaps. Biosystems Engineering. 2013;114(4):358-371.
15. Weiss M, Jacob F, Duveiller G. Remote sensing for agricultural applications: a meta-review. Remote Sensing of Environment. 2020;236:111402.
16. Basso B, Antle J. Digital agriculture to design sustainable agricultural systems. Nature Sustainability. 2020;3(4):254-256.
17. Kayad A, Sozzi M, Gatto S, Marinello F, Pirotti F. Monitoring within-field variability of corn yield using Sentinel-2 and machine learning techniques. Remote Sensing. 2019;11(23):2873.
18. Yost MA, Hartemink AE. Soil fertility mapping and management for precision agriculture: a review. Advances in Agronomy. 2019;158:39-104.
19. Shukla AK, Mishra T, Tripathi KM, Kumar A, Yadav K. Site-specific nutrient management: an overview and its applicability under Indian conditions. Indian Journal of Fertilisers. 2020;16(10):1010-1023.

20. Sishodia RP, Ray RL, Singh SK. Applications of remote sensing in precision agriculture: a review. Remote Sensing. 2020;12(19):3136.
21. Bwambale E, Abagale FK, Anornu GK. Smart irrigation monitoring and control strategies for improving water use efficiency in precision agriculture: a review. Agricultural Water Management. 2022;260:107324.
22. Jha K, Doshi A, Patel P, Shah M. A comprehensive review on automation in agriculture using artificial intelligence. Artificial Intelligence in Agriculture. 2019;2:1-12.
23. Sharma A, Jain A, Gupta P, Chowdary V. Machine learning applications for precision agriculture: a comprehensive review. IEEE Access. 2021;9:4843-4873.
24. Mahajan GR, Das B, Murgaokar D, Herrmann I, Berger K, Sahoo RN, *et al*. Monitoring the foliar nutrients status of mango using spectroscopy-based spectral indices and machine learning models. Remote Sensing. 2021;13(4):641.
25. Say SM, Keskin M, Sehri M, Sekerli YE. Adoption of precision agriculture technologies in developed and developing countries. Online Journal of Science and Technology. 2018;8(1):7-15.
26. Dhillon R, Moncrief J. Sensor-based site-specific nitrogen application in row crops: a review. Computers and Electronics in Agriculture. 2021;185:106126.
27. Bongiovanni R, Lowenberg-DeBoer J. Precision agriculture and sustainability. Precision Agriculture. 2004;5(4):359-387.
28. Khanal S, Fulton J, Shearer S. An overview of current and potential applications of thermal remote sensing in precision agriculture. Computers and Electronics in Agriculture. 2017;139:22-32.
29. Food and Agriculture Organization of the United Nations. The Future of Food and Agriculture: Trends and Challenges. Rome: Food and Agriculture Organization of the United Nations; c2018.